DETECTION OF TRIPLY DEUTERATED AMMONIA IN THE BARNARD 1 CLOUD

D. C. LIS,[1] E. ROUEFF,[2] M. GERIN,[3] T. G. PHILLIPS,[1] L. H. COUDERT,[4] F. F. S. VAN DER TAK,[5] AND P. SCHILKE[5]

ABSTRACT

We report the detection of the ground-state rotational transition $J_K = 1_0 \rightarrow 0_0$ ($0a \rightarrow 0s$) of triply deuterated ammonia at 309.91 GHz in the Barnard 1 cloud, obtained with the Caltech Submillimeter Observatory. The observed, integrated, line intensity of 0.307 ± 0.019 K km s^{-1} implies an ND$_3$ column density of $(2 \pm 0.9) \times 10^{12}$ cm^{-2}, for excitation temperatures in the range 5–10 K. Using previously published H$_2$ and NH$_3$ column density estimates in this source, we derive an ND$_3$ fractional abundance with respect to H$_2$ of $(1.5 \pm 1) \times 10^{-11}$ and an ND$_3$-to-NH$_3$ abundance ratio of $\sim 8 \times 10^{-4}$. The observed abundance ratios can be explained in the framework of gas-phase chemical models, in which the dissociative recombination of partially deuterated ions results in a somewhat higher probability for the ejection of hydrogen atoms than deuterium.

Subject headings: ISM: abundances — ISM: individual (Barnard 1) — ISM: molecules

1. INTRODUCTION

The initial detection of deuteration in heavy molecules in the interstellar medium (ISM) was for HCN (Jefferts, Penzias, & Wilson 1973), where DCN was found to be 6×10^{-3} of HCN (Wilson et al. 1973), compared to the local ISM D/H ratio of $(1.5 \pm 0.1) \times 10^{-5}$ (Wilson 1999 and references therein). This surprising result was explained by chemical fractionation under low-temperature conditions (Solomon & Woolf 1973). Recent detections of doubly deuterated ammonia and formaldehyde in L134N and L1689N (Roueff et al. 2000; Ceccarelli et al. 1998; Loinard et al. 2001) have renewed interest in deuterium fractionation in cold, dense molecular gas. The concept of the detection of triply deuterated species was, until now, so remote that the lines were omitted from the line catalogs for astrophysics, even though laboratory-measured frequencies were available. Amazingly, under the right conditions, ND$_3$ can indeed be detected, providing clues to the physics of the dense, cold ISM.

ND$_3$ is a symmetric top molecule with the energy diagram similar to that of NH$_3$ (see, e.g., Fig. 12-10 of Bunker 1979). However, owing to the difference in nuclear spin between the proton and deuteron, the levels in the $K = 0$ ladder that in the case of NH$_3$ are only populated for odd J-values in the inversion s-state and for even J-values in the inversion a-state (see Fig. 12-10 of Bunker 1979) are all populated in the case of ND$_3$. Consequently, the ND$_3$ $J_K = 1_0 \rightarrow 0_0$ transition is split into two components, $0a \rightarrow 0s$ and $0s \rightarrow 0a$, by the inversion.[6] The statistical weight ratio of the two components due to the nuclear spin is 10 : 1 (see Table 3-6 of Townes & Schawlow 1975). Each of the two components is further split by the ^{14}N quadrupole coupling into a closely spaced triplet with the statistical weight ratios of 3 : 5 : 1. The submillimeter spectrum of ND$_3$ was first measured in the laboratory by Helminger & Gordy (1969), and

the computational estimates of the line frequencies given in Table 1 are based on the later work of Fusina, Di Lonardo, & Johns (1985) for the rovibrational constants and the work of Ruben & Kukolich (1974) for the hyperfine coupling constants.

Chemical models indicate that highest deuterium fractionation levels occur in cold, high-density regions. The best targets to search for ND$_3$ are thus high column density condensations in dark clouds without embedded luminous sources. Barnard 1 is one of the highest column density molecular sources in the Perseus complex. Bachiller, Menten, & del Río-Alvarez (1990) presented a comprehensive study of this region in a variety of molecular tracers. The presence of several low-luminosity *IRAS* sources indicates some ongoing low-mass star formation. Interferometric observations of Hirano et al. (1997) suggest that the *IRAS* source 03301+3057, located within the dense NH$_3$ core, is a protostellar candidate, in an early evolutionary stage, having a molecular outflow in a nearly pole-on configuration. Hirano et al. (1999) derive an H^{13}CO$^+$ fractional abundance a factor of 3–4 lower than the canonical value (Frerking, Langer, & Wilson 1987), indicating significant depletions of gas molecules (^{13}CO) onto the dust grains.

The low kinetic temperature and high density make Barnard 1 an excellent target for studies of multiply deuterated molecular species. We present here results of a sensitive search for the ground-state rotational line of ND$_3$ in this source, which, together with separate observations of NGC 1333 (van der Tak et al. 2002), constitute the first astrophysical detection of a triply deuterated molecule.

2. OBSERVATIONS

Spectroscopic observations of the Barnard 1 cloud presented here were carried out in 2002 February using the 345 and 230 GHz facility receivers and spectrometers of the Caltech Submillimeter Observatory (CSO) on Mauna Kea, Hawaii. The data were taken under average weather conditions (225 GHz zenith opacity $\sim$0.06–0.18). CSO FWHM beam size at 309 GHz is $\sim$25″, and the main-beam efficiency at the time of the observations, determined from total-power observations of Mars and Saturn, was $\sim$60%. Typical calibration uncertainties are $\sim$25%. The pointing of the telescope was stable to within $\lesssim$5″. We used the 1.5 GHz, 500 MHz, and 50 MHz bandwidth acousto-optical facility spectrometers. The spectral resolution of the high-resolution, 1024-channel 50 MHz bandwidth spectrometer, measured from a frequency comb scan, was 3.4 spectral channels,

[1] Downs Laboratory of Physics, California Institute of Technology, MS 320-47, Pasadena, CA 91125; dcl@submm.caltech.edu.

[2] Laboratoire Univers et Théorie, FRE 2462 du CNRS, Observatoire de Paris, Section de Meudon, Place Jules Janssen, 92195 Meudon, France.

[3] Laboratoire d'Etude du Rayonnement et de la Matière en Astrophysique, FRE 2460 du CNRS, Observatoire de Paris and Ecole Normale Supérieure, 24 Rue Lhomond, 75231 Paris Cedex 05, France.

[4] Laboratoire de Photophysique Moléculaire, CNRS, Batiment 350, Universite Paris-Sud, 91405 Orsay, France.

[5] Max-Planck-Institut für Radioastronomie, Auf dem Hügel 69, D-53121 Bonn, Germany.

[6] The corresponding NH$_3$ transition at 572.5 GHz was first detected in the ISM by Keene, Blake, & Phillips (1983).

TABLE 1
COMPUTED FREQUENCIES OF THE ND_3
HYPERFINE COMPONENTS

Transition	ν (GHz)	Strength
$J_K = 1_0 \rightarrow 0_0$ $(0s \rightarrow 0a)$		
$F = 1-1$	306.7353031	0.058
$F = 2-1$	306.7365301	0.097
$F = 0-1$	306.7383706	0.019
$J_K = 1_0 \rightarrow 0_0$ $(0a \rightarrow 0s)$		
$F = 1-1$	309.9081112	0.60
$F = 2-1$	309.9093382	1.00
$F = 0-1$	309.9111787	0.20

or 0.16 MHz. The 50 and 500 MHz spectrometers give consistent line intensities, typically within ≲5%–10%. However, the 1.5 GHz spectrometer, which offers the largest spectral bandwidth, suffers intensity calibration errors due to power compression. Consequently, an empirical scaling factor of 0.82 was applied to the 1.5 GHz data presented here. All the spectra were taken in the beam-switched observing mode with a secondary chopper throw of 180″.

3. RESULTS

Figure 1 shows the distribution of the DCO⁺ (3–2) emission in Barnard 1 that can be used as an indicator of the approximate spatial distribution of other deuterated molecular species. The FWHM CSO beam for the ND_3 observations described here, shown as a dotted circle, encompasses the two compact millimeter continuum sources (Hirano et al. 1999).

3.1. *Line Identification*

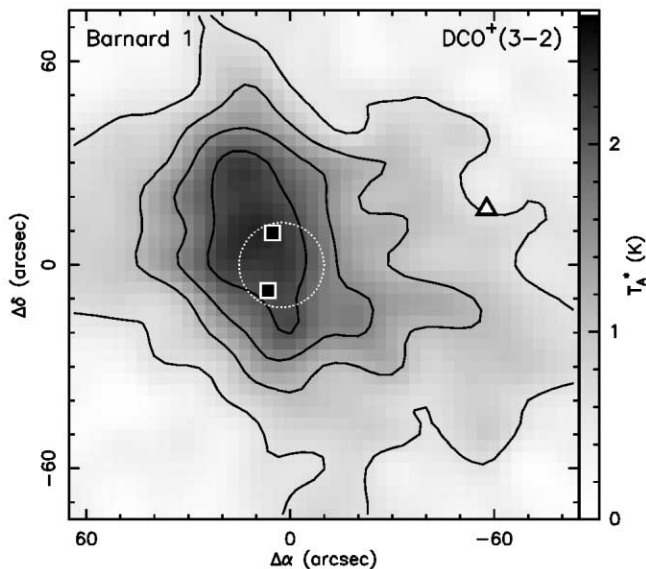Since the CSO facility receivers operate in double-sideband mode, two spectra taken with different frequency settings are

FIG. 1.—Gray-scale image of the DCO⁺ (3–2) intensity in Barnard 1 integrated over the 5.5–8 km s⁻¹ velocity range at a 35″ angular resolution, observed with the 230 GHz CSO facility receiver. Contour levels are 25%, 45%, 65%, and 85% of the peak integrated intensity, 2.47 K km s⁻¹ (T_A^*). Symbols mark the locations of the *IRAS* source 03301+3057 (*triangle*) and the 3 mm continuum sources (*squares*; Hirano et al. 1999). FWHM size of the CSO beam at 309 GHz is shown as a dotted circle. Offsets, in units of arcseconds, are relative to the position $\alpha_{1950} = 3^h30^m15^s$, $\delta_{1950} = 30°57'30''.5$.
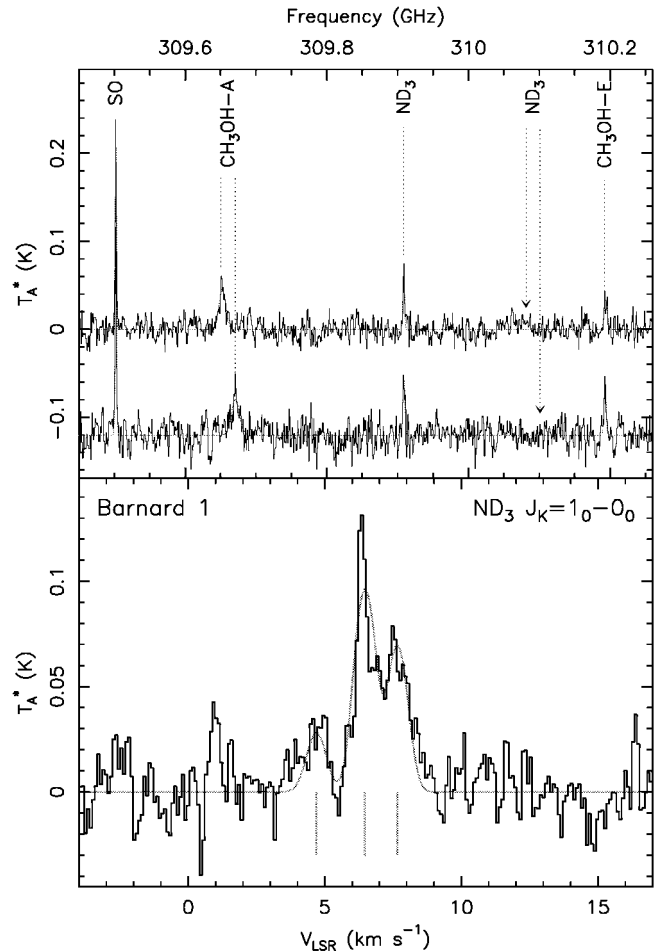

FIG. 2.—*Upper panel*: Low-resolution spectra of the 309.91 GHz ND_3 transition taken with the 1.5 GHz spectrometer for two frequency settings shifted by 10 MHz. Three of the four spectral features seen in the spectra can be identified with transitions of SO, CH_3OH–A, and CH_3OH–E with the help of the JPL line catalog. The absence of a frequency shift between the two spectra uniquely assigns the 309.91 GHz feature to the signal sideband. Vertical arrows mark the location of the 306.74 GHz ND_3 line in the image sideband. A 3 σ lower limit of ~4.3 for the intensity ratio of the 309.91–306.73 GHz ND_3 lines is consistent with the optically thin ratio of 10 : 1. *Lower panel*: High-resolution spectrum of the 309.91 GHz ND_3 line taken with the 50 MHz spectrometer. The total integration time of 78 minutes on-source resulted in an rms noise level of 17 mK after Hanning-smoothing the spectrum once (0.094 km s⁻¹ channel width). The hyperfine structure fit obtained using the frequencies given in Table 1 is shown as a thin solid line.

required to uniquely assign a line of interest to the signal or image sideband. Figure 2 (*upper panel*) shows low-resolution spectra, taken with the 1.5 GHz spectrometer, for two frequency settings shifted by 10 MHz. Of the four spectral features seen in the spectrum, three, including the 309.91 GHz line, show no frequency shift and are assigned to the signal sideband. One shows a 20 MHz shift and is assigned to the image sideband, where, with the help of the JPL line catalog (Pickett et al. 1998), it is found to be the CH_3OH–A $(4_{32}–4_{22})$ line with a lower level energy of 23.2 K. Two other lines in the signal sideband are assigned to SO $(2_2–1_2)$ with a lower level energy of 4.5 K and CH_3OH–E $(3_{21}–2_{11})$ with a lower level energy of 19.9 K. ND_3 is the identification for the 309.91 GHz spectral feature.

Figure 2 (*lower panel*) shows a high-resolution spectrum of the 309.91 GHz line taken with the 50 MHz spectrometer. No lines within 5 MHz of the frequency of the emission peak are found in the JPL line catalog. The hyperfine structure fit, obtained using the computed ND_3 line frequencies and intensity

TABLE 2
MOLECULAR COLUMN DENSITIES AND ABUNDANCES IN BARNARD 1

Molecule	N	X	Model A	Model B
H_2	1.3×10^{23}	1	1	1
CO	3.9×10^{18}	3×10^{-5}	2.6×10^{-5}	2.6×10^{-5}
NH_3	2.5×10^{15}	1.9×10^{-8}	2.1×10^{-8}	2.1×10^{-8}
NH_2D	...	...	2.7×10^{-9}	2.9×10^{-9}
ND_2H	...	...	6.9×10^{-11}	1.5×10^{-10}
ND_3	2.0×10^{12}	1.5×10^{-11}	1.8×10^{-12}	1.2×10^{-11}
ND_3/NH_3	...	8×10^{-4}	9×10^{-5}	6×10^{-4}

ratios given in Table 1, is shown as a gray line. Features at the frequencies of the two strongest ND_3 hyperfine components are clearly detected in the spectrum at $\gtrsim 5 \sigma$ level in a single channel. The weakest component is also probably detected. The fit gives a line center velocity of 6.47 ± 0.04 km s^{-1}, an FWHM line width of 0.82 ± 0.07 km s^{-1}, and a line center optical depth of the strongest component of 1.1 ± 0.8. The line center velocity and line width given by the fit agree to within 0.3 and 0.05 km s^{-1}, respectively, with those of the NH_3 inversion line in Barnard 1 (Bachiller et al. 1990).

Given the absence of any alternative candidate lines in the JPL line catalog, the characteristic line shape consistent with the ND_3 hyperfine splitting, and the velocity agreement with other molecular species in Barnard 1, we confidently identify the spectral feature at 309.91 GHz with the $J_K = 1_0 \rightarrow 0_0$ $(0a \rightarrow 0s)$ ground-state rotational transition of ND_3. The possibility of the feature being an uncataloged, excited-state line of an ISM molecule is very low owing to the low kinetic temperature of the medium.

3.2. ND_3 Column Density and Fractional Abundance

The observed ND_3 integrated line intensity in the 5.5–8.5 km s^{-1} velocity range (which includes the two strongest hyperfine components) is 0.164 ± 0.010 K km s^{-1}. Correcting for the intensity of the weakest hyperfine component and applying a 60% main-beam efficiency, we derive an integrated line intensity of 0.307 ± 0.019 K km s^{-1} for the ND_3 $J_K = 1_0 \rightarrow 0_0$ $(0a \rightarrow 0s)$ line.

The column density of ND_3 is given by

$$N_{\text{tot}} = \frac{8\pi\nu^3}{c^3} \frac{Q(T_{\text{ex}})}{g_u A} \frac{e^{E_u/kT_{\text{ex}}}}{e^{h\nu/kT_{\text{ex}}} - 1} \int \tau \, dv, \qquad (1)$$

where ν is the line frequency, $Q(T)$ is the partition function, T_{ex} is the excitation temperature, g_u is the upper level degeneracy including the statistical weight due to the nuclear spin, A is the Einstein spontaneous emission coefficient, E_u is the upper level energy, and τ is the optical depth. The optical depth is not adequately constrained by the hyperfine structure fit, which is consistent with optically thin emission. Therefore, we derive the optical depth from the observed line intensity using the formula $T_R = [J_\nu(T_{\text{ex}}) - J_\nu(T_{\text{bg}})](1 - e^{-\tau})$, where $J_\nu(T) = (h\nu/k)/(e^{h\nu/kT} - 1)$ is the radiation temperature of a blackbody at a temperature T, and T_{bg} is the cosmic background temperature (2.7 K). In the optically thin case, $\tau = T_R/[J_\nu(T_{\text{ex}}) - J_\nu(T_{\text{bg}})]$, and equation (1) can be written as

$$N_{\text{tot}} = \frac{8\pi k\nu^2}{hc^3} \frac{Q(T_{\text{ex}})}{g_u A} e^{E_u/kT_{\text{ex}}} \frac{1}{1 - [J_\nu(T_{\text{bg}})/J_\nu(T_{\text{ex}})]} \int T_R \, dv. \qquad (2)$$

Based on their NH_3 observations with the Effelsberg telescope (~40″ beam), Bachiller et al. (1990) derive an NH_3 column density of ~2.5×10^{15} cm^{-2}, a kinetic temperature

$T_k = 12$ K in the high column density regions, and a volume density $n_{H_2} = 7 \times 10^4$ cm^{-3} in Barnard 1. The lack of knowledge of the collisional cross sections for ND_3 and the limited signal-to-noise ratio in the observed ND_3 spectrum prevent us from accurately determining the excitation temperature. Gerin et al. (2001) derive an N_2D^+ (3–2) excitation temperature of 4.4 K from a hyperfine structure fit. Given our present knowledge of the physical conditions in the Barnard 1 core, an ND_3 excitation temperature in the range 5–10 K is justified.

In the case of the ND_3 $J_K = 1_0 \rightarrow 0_0$ $(0a \rightarrow 0s)$ transition, $\nu = 309.9091337$ GHz, $g_u = 30$, $A = 2.516 \times 10^{-4}$ s^{-1}, $E_u = 14.87$ K, and $Q(10 \text{ K}) = 38.30$. Therefore, for this value of the excitation temperature, the observed integrated line intensity of 0.307 ± 0.019 K km s^{-1} leads to an ND_3 column density of $(1.3 \pm 0.3) \times 10^{12}$ cm^{-2}, assuming a 25% calibration uncertainty (3σ). The derived ND_3 column density depends critically on the assumed value of the excitation temperature. For a 5 K excitation temperature, the partition function $Q(5 \text{ K}) = 17.23$, and the corresponding ND_3 column density is $(2.8 \pm 0.7) \times 10^{12}$ cm^{-2}. Our final estimate of the ND_3 column density toward Barnard 1 is thus $(2 \pm 0.9) \times 10^{12}$ cm^{-3} (3σ), where the uncertainty includes both the calibration and modeling uncertainties, due to the unknown excitation temperature, added in quadrature.

Hirano et al. (1999) derive H_2 column densities of ~$(1.3$– $1.5) \times 10^{23}$ cm^{-2}, in a 15″ beam, along the ridge connecting the two millimeter continuum sources in Barnard 1, based on their observations of the 850 μm dust continuum emission. The position we have observed is within ~10″ of the two continuum peaks. Taking 1.3×10^{23} cm^{-2} as an estimate of the H_2 column density within our beam, we derive an ND_3 fractional abundance of $(1.5 \pm 1) \times 10^{-11}$, where the uncertainty includes a 50% uncertainty in the H_2 column density added in quadrature to the uncertainty of the ND_3 column density derived above. Using the NH_3 column density of 2.5×10^{15} cm^{-2} (Bachiller et al. 1990), we derive an ND_3/NH_3 abundance ratio of 8×10^{-4}. Table 2 gives a summary of the molecular column densities and fractional abundances in Barnard 1.

3.3. CO Abundance in Barnard 1

As discussed by Tiné et al. (2000), abundances of multiply deuterated ammonia in gas-phase chemical models depend on the elemental depletion of carbon and oxygen relative to nitrogen. The observed abundance of CO, an important reservoir of carbon and oxygen in the gas phase, can thus be used as an observational constraint for the chemical models. To estimate the CO abundance in Barnard 1, we use $C^{18}O$ and $C^{17}O$ (2–1) spectra obtained with the IRAM 30 m telescope (~11″5 beam; E. Roueff et al. 2002, in preparation).

Large velocity gradient (LVG) modeling, assuming a 12 K kinetic temperature and 7×10^4 cm^{-3} volume density (Bachiller et al. 1990), gives a $C^{18}O$ column density of 7×10^{15} cm^{-2} and a line center optical depth of ~1.3.

We also derive a $C^{17}O$ column density of 1.8×10^{15} cm^{-2} and a line center opacity of 0.2. The $C^{18}O$-to-$C^{17}O$ abundance ratio of 3.8 is consistent with the average $^{18}O/^{17}O$ isotopic ratio of 3.6 ± 0.2 for the local ISM sources (Wilson 1999). With an H_2 column density of 1.3×10^{23}, we derive a $C^{18}O$ fractional abundance relative to H_2 of 5.4×10^{-8}, a factor of ~3 lower than the canonical value (Frerking, Langer, & Wilson 1982).

Assuming a standard $^{16}O/^{18}O$ isotopic ratio of 557 in the local ISM (Wilson 1999), we derive a CO fractional abundance of 3×10^{-5} relative to H_2, indicating that a significant fraction of CO molecules is frozen onto the dust grains.

4. CHEMISTRY OF ND$_3$

Rodgers & Charnley (2001) suggested that ND$_3$ may be produced either by grain surface or gas-phase chemistry. However, in the absence of quantitative estimates of surface reactions, we have developed a gas-phase chemical model, in which all the deuterium-substituted versions of NH, NH$_2$, NH$_3$, and the corresponding ions, NH$^+$, NH$_2^+$, NH$_3^+$, and NH$_4^+$, have been included, as well as D$_2$, D$_2$H$^+$, and D$_3^+$. Only monodeuterated species of oxygen and carbon molecules have been considered at the present time. As a result, 152 species are linked by about 1800 gas-phase chemical reactions. As stressed by several authors (e.g., Roberts & Millar 2000a, 2000b), the first step in deuteration of interstellar molecules relies on the fractionation reaction between H$_3^+$ and HD. We have introduced the recent low-temperature reaction rate coefficients obtained in a trap experiment (Gerlich, Herbst, & Roueff 2002), where the successive reactions of H$_3^+$ and its deuterated substitutes with HD and D$_2$ have been measured. We assume that H$_2$ is entirely para, so that deuteration proceeds efficiently. With these assumptions, triply deuterated ammonia is formed essentially from dissociative recombination of NHD$_3^+$, where we follow the usual rules to extend a standard chemistry to deuterated species (e.g., Roberts & Millar 2000a). We have introduced the most recent branching ratios from the available storage ring experiments as reviewed by Le Petit & Roueff (2002). Nevertheless, many unknown reaction rate coefficients remain in the chemical network.

Table 2 gives the steady-state molecular abundances, relative to H$_2$, obtained from our chemical network. We have taken the various constraints derived from the observations, i.e., density (7×10^4 cm^{-3}), temperature (12 K), and elemental depletion consistent with the CO abundance derived above. Model A refers to a chemical network where the standard assumptions of statistical ratios are used for the various reactions, when they are not measured. However, the available experimental determinations of the branching ratios have shown that this latter approximation is rarely fulfilled (see, for example, the dissociative recombination of NH$_4^+$ by Vikor et al. 1999). Moreover, the ejection of the light hydrogen atom is favored in comparison to atomic deuterium for deuterated ions such as H$_2$D$^+$. We have thus considered a chemical network, B, where we specifically assume that the dissociative recombination results in the ejection of H atoms with a 75% probability, compared to 25% for deuterium (experiments have shown ratios of about 2 : 1 for the ejection probability of H and D in triatomic ions; Le Petit & Roueff 2002). The enhanced deuterium branching ratios in model B are used for all dissociative recombination reactions, except those that have been measured in the laboratory (i.e., those involving H$_2$D$^+$, D$_3^+$, H$_2$O$^+$, HDO$^+$).

The results are extremely sensitive to the assumptions for the dissociative recombination, as shown in Table 2. It should also be stressed that the results depend on the gas density, temperature, and elemental depletion. It is thus encouraging that a good agreement with the observations is obtained for the physical conditions derived previously for the Barnard 1 core. The rate coefficient of the reaction between H$_3^+$ and HD also plays a key role in the deuterium chemistry. Using the collisional value, instead of that measured by Gerlich et al. (2002), results in high fractionation of ammonia without the need for enhanced branching ratios for the retention of D atoms. The corresponding ND$_3$ abundance is 3.7×10^{-11}. A more detailed discussion of the ND$_3$ chemistry, beyond the scope of this Letter, will be presented elsewhere (E. Roueff et al. 2002, in preparation). Here we can only state that the observed ND$_3$ abundance ($\sim 1.5 \times 10^{-11}$) and the ND$_3$-to-NH$_3$ abundance ratio in Barnard 1 ($\sim 8 \times 10^{-4}$) are consistent with predictions of gas-phase chemical models, as long as the dissociative recombination of deuterated ions results in hydrogen atoms being ejected with a higher probability than the deuterium atoms. However, we cannot exclude the possibility that surface processes also contribute to the formation of ND$_3$ (see Rodgers & Charnley 2001). Searches for NH$_2$D and ND$_2$H on the same line of sight are urgent objectives, and determination of relative abundances of the isotopic variants will help to constrain the chemical processes at work.

REFERENCES

Bachiller, R. Menten, K. M., & del Río-Alvarez, S. 1990, A&A, 236, 461
Bunker, P. R. 1979, Molecular Symmetry and Spectroscopy (New York: Academic)
Ceccarelli, C., Castets, A., Loinard, L., Caux, E., & Tielens, A. G. G. M. 1998, A&A, 338, L43
Frerking, M. A., Langer, W. D., & Wilson, R. W. 1982, ApJ, 262, 590
———. 1987, ApJ, 313, 320
Fusina, L., Di Lonardo, G., & Johns, J. W. C. 1985, J. Mol. Spectrosc., 121, 211
Gerin, M., et al. 2001, ApJ, 551, L193
Gerlich, D., Herbst, E., & Roueff, E. 2002, Planet. Space Sci., submitted
Helminger, P., & Gordy, W. 1969, Phys. Rev., 188, 100
Hirano, N., Kamazaki, T., Mikami, H., Ohashi, N., & Umemoto, T. 1999, in Star Formation 1999, ed. T. Nakamoto (Nagano: NRO), 181
Hirano, N., Kameya, O., Mikami, H., Saito, S., Umemoto, T., & Yamamoto, S. 1997, ApJ, 478, 631
Jefferts, K. B., Penzias, A. A., & Wilson, R. W. 1973, ApJ, 179, L57
Keene, J., Blake, G. A., & Phillips, T. G. 1983, ApJ, 271, L27
Le Petit, F., & Roueff, E. 2002, in Dissociative Recombination of Molecular Ions with Electrons, ed. S. Guberman (New York: Kluwer/Plenum), in press

Loinard, L., Castets, A., Ceccarelli, C., Caux, E., & Tielens, A. G. G. M. 2001, ApJ, 552, L163
Pickett, H. M., Poynter, R. L., Cohen, E. A., Delitsky, M. L., Pearson, J. C., & Müller, H. S. P. 1998, J. Quant. Spectrosc. Radiat. Transfer, 60, 883
Roberts, H., & Millar, T. J. 2000a, A&A, 361, 388
———. 2000b, A&A, 364, 780
Rodgers, S. D., & Charnley, S. B. 2001, ApJ, 553, 613
Roueff, E., Tiné, S., Coudert, L. H., Pineau des Forêts, G., Falgarone, E., & Gerin, M. 2000, A&A, 354, L63
Ruben, D. J., & Kukolich, S. G. 1974, J. Chem. Phys., 61, 3780
Solomon, P. M., & Woolf, N. J. 1973, ApJ, 180, L89
Tiné, S., Roueff, E., Falgarone, E., Gerin, M., & Pineau des Forêts, G. 2000, A&A, 356, 1039
Townes, C. H., & Schawlow, A. L. 1975, Microwave Spectroscopy (New York: Dover)
van der Tak, F. F. S., Schilke, P., Müller, H. S. P., Lis, D. C., Phillips, T. G., & Gerin, M. 2002, A&A, submitted
Vikor, L., et al. 1999, A&A, 344, 1027
Wilson, R. W., Penzias, A. A., Jefferts, K. B., & Solomon, P. M. 1973, ApJ, 179, L107
Wilson, T. L. 1999, Rep. Prog. Phys., 62, 143